An Electrically Driven Gas Compressor for Hydrogen Refueling Stations with Active Power Smoothing

Alfred Rufer
EPFL Ecole Polytechnique Fédérale de Lausanne
STI-DO-EPFL Station 11
CH1015 Lausanne, Switzerland
+4179 244 09 84
alfred.rufer@epfl.ch

Keywords

«Electrical drive», « Active power-decoupling circuit», « Capacitors», « Highly dynamic drive», « Force Control»

Abstract

A new electrically driven gas booster is described as an alternative to the classical air-driven gas boosters known for their poor energetic efficiency. These boosters are used in hydrogen refueling stations where the global energy account is of significancy. The proposed system uses a common crankshaft and two connecting rods to transform the rotational motion of the motor to the linear displacement of the original compressor pistons. The strongly fluctuating power of the compressor is smoothed by an active capacitive auxiliary storage device connected to the DC circuit of the power converter that feeds the electric motor.
The paper describes the typical behaviour of the compressor and of the coupling mechanism from the point of view of the needed forces, torques and power. The design of the auxiliary storage capacitor is given and the very specific waveforms are represented.

Introduction

Green Hydrogen is a promising energy vector in the sector of automotive vehicles especially in the context of reducing the emissions of green-house gases. Due to its low weight density, Hydrogen must be stored on-board in high pressure reservoirs. A simplified representation of a Green Hydrogen refueling station is given in Fig. 1. In such a system, the green fuel is generated from electric renewable source feeding a water electrolyser.

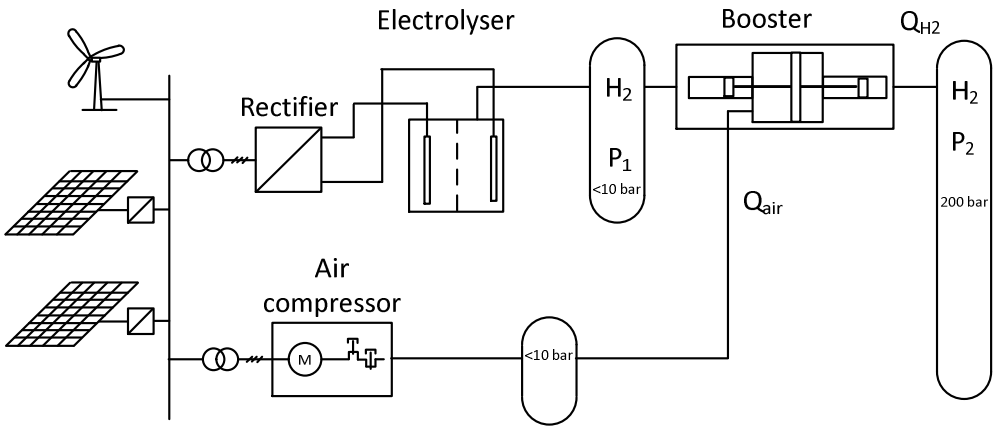

Fig. 1 Example of a Hydrogen refueling station for automotive vehicles.

Then, the green fuel is pressurized to a high-pressure level around 700 bar for personal vehicles or 350 bar for heavy transportation means. The pressurization machinery is realized conventionally by air driven gas boosters which are known for their simplicity, reliability and low costs [1].
However, the poor energetic efficiency of the used pneumatic motor in the gas booster addresses the question of the total efficiency of a complete filling station. In general, the main cause of the poor efficiency of pneumatic actuators resides in the fact that the air under pressure accumulated in the working chambers is simply released to the surrounding before initiating the return stroke. Fig. 2 shows a pressure-to-volume diagram of the thermodynamic change of state of the air in a pneumatic cylinder, where the constant pressure displacement work is represented with the finely hatched square surface W_2 between V_1 and V_2. This surface corresponds to the effectively produced mechanical work by a cylinder under constant pressure P_2. Left to the V_2 value of the volume, the surface under the decreasing curve (W_{2d}) corresponds to the recoverable expansion work corresponding to the lost energy when the exhaust valve is opened.

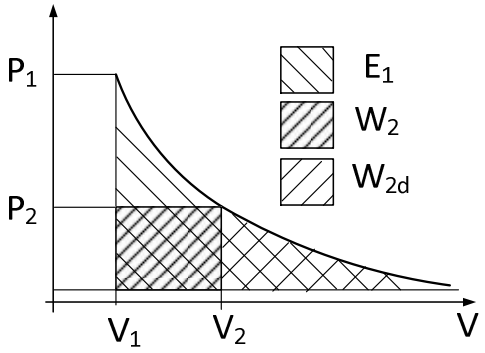

Fig. 2 Pressure-volume diagram of pressurized air work and expansion

A better use of the pressurized air of a cylinder has been proposed, using the principle of adding an expansion work component to the constant pressure displacement work, recovering so the internal energetic content of the intaken air [2-5]. In principle, the addition of an expansion chamber can increase the cylinder system efficiency from around 0.35 to 0.7 [4]. With the same goal to improve the efficiency, the principle of using the expansion energy has been applied to a pneumatic booster [6]. Another better adapted system is based on the use of an additional expansion cylinder mechanically coupled to the filling cylinder [7]. The resultant active force is in this case better adapted to the compression characteristic but needs a specific design to be able to provide a sufficient effort over the full length of the strokes.

In this paper, an electrically driven gas booster is proposed, where the mechanical force is provided by a classical electric motor. The coupling of the rotational motion of the motor to the linear displacement of the compression stages is realized on the base of a classical crankshaft and two connecting rods. The original compression cylinders are conserved and placed on both sides of the crankshaft. The strongly fluctuating compression force of the pistons at a low frequency results in a strongly modulated power of the electric motor. For smoothing the power taken from the electrical feeding grid, an active power compensation system using variable voltage capacitors is connected to the DC link of the frequency converter.

An electric motor instead of the common pneumatic actuator

Figure 3 shows on the top the classical air-driven gas booster with the complete feeding chain which comprises an electric motor driving an air compressor. The pressurized air reservoir serves not only as a simple power source for the air-drive of the compressor but plays additionally the role of power buffer for the strongly fluctuating power demand of the compression cylinders. The cascade of the

partial efficiencies of the electric motor (87%), the air compressor (65%) and a classical pneumatic booster (35%) leads to a compression efficiency of around 20%.

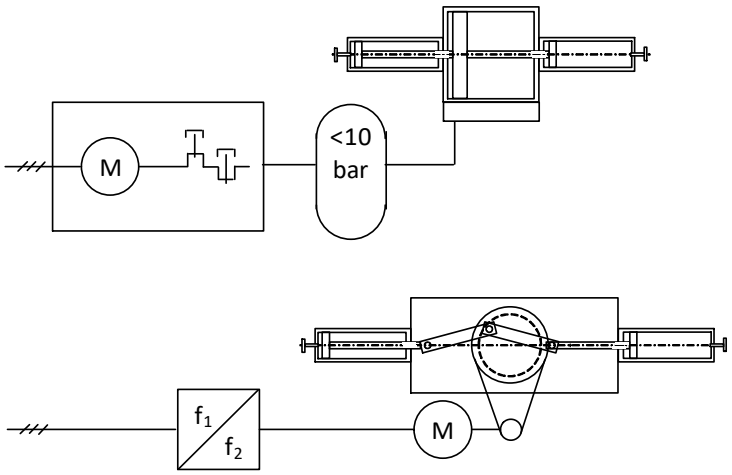

Fig. 3 Gas booster driven by a crankshaft and two connecting rods

In the lower part of the figure, the new proposed system is represented where the motion of the compression cylinders is provided by a crankshaft and two connecting rods driven by a variable frequency rotating field machine. The low operating frequency of the compression stages is determined by the temperature limit of the compression stages and needs to insert a mechanical reduction gear between motor and crankshaft. This new system greatly simplifies the supply chain of the compression stages by reducing the number of successive energy conversions and by eliminating the pneumatic compressor and actuator. The result is a highly improved energy efficiency. The partial efficiencies are estimated as 95% for the frequency converter, 92% for the motor and 97% for the gear, leading to a value of 84% for the driving equipment.
Regarding the strongly fluctuating power demand of the cylinders, the frequency converter is equipped with an active power compensation stage based on a capacitive storage circuit.

Coupling the rotational motion to the linear displacement of the pistons

The most known method for coupling a rotational motion to a linear displacement is given by the classical crankshaft system. In the proposed system, the alternating operation of a left and right compression cylinders is maintained. The crankpin is therefore coupled to two separated connecting rods (bottom of Fig. 3).

Mathematical description of the piston-crankshaft assembly

In Figure 4 a piston assembly is represented with the connecting rod and the crankshaft. The parameters are indicated as r, the radius of the crankshaft, l the length of the connecting rod, and Φ the angle of rotation of the crankshaft. The diameter of the piston, d and its position x are also indicated.

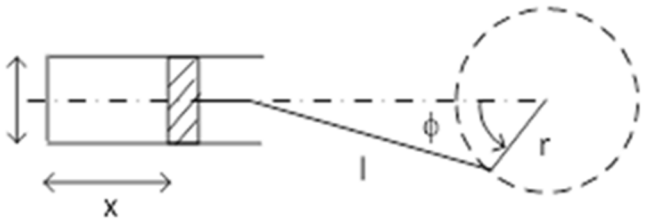

Fig. 4 Piston, crankshaft and connecting rod

The position of the piston is given through rel. (1)

$$x = r(1-\cos\varphi) + \frac{\lambda}{2} r \sin^2\varphi \tag{1}$$

where the connecting rod ratio λ is used and is defined as

$$\lambda = \frac{r}{l} \tag{2}$$

The velocity of the piston is given by

$$v = \omega \cdot r \cdot \sin\varphi(1 + \lambda\cos\varphi) \tag{3}$$

In the simulation process, the torque developed by the motor is calculated through the indirect calculation of the power. If the force exerted on the piston is given by

$$F_p = p \cdot A \tag{4}$$

the mechanical power is defined by the product of the force by the piston's velocity:

$$Pow = F_p \cdot v \tag{5}$$

The torque is obtained by the division of the power by the angular velocity ω

$$M_{mot} = Pow / \omega \tag{6}$$

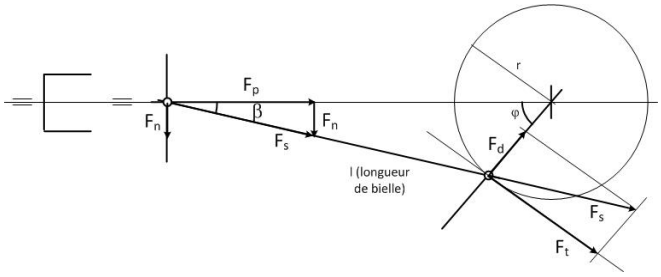

Fig. 5 Diagram of the forces for the calculation of the torque and reactions

A direct calculation of the torque is however possible with the extended model represented in Fig. 5 [8]. The force on the connecting rod F_s, the tangential force F_t and the reaction force F_n are also defined. The torque on the crankshaft is given by rel.7.

$$M_{mot} = F_t \cdot r \tag{7}$$

The tangent force F_t is given by (8)

$$F_t = F_s \cos(\pi/2 - (\beta + \varphi)) \tag{8}$$

The force transmitted through the connecting rod F_s is calculated with the help of the piston force F_p and the angle beta (9)

$$F_s = \frac{F_p}{\cos\beta} \tag{9}$$

This angle is given by rel. (10)

$$\beta = arc\sin\left(\frac{r}{l} \cdot \sin\varphi\right) \tag{10}$$

The perpendicular reaction F_n is defined as per (11)

$$F_n = F_s \sin\beta = \frac{F_p}{\cos\beta}\sin\beta \tag{11}$$

Simulation results

In Figure 6, the dimensionless evolution of the volumes of the compression cylinders is represented. The blue curve is representing the evolution of the left cylinder while the red curve shows the behaviour of the right cylinder. The curves represent already the asymmetric variation of the volumes of the left and right compression cylinders due to properties of the used crankshaft and 180° shifted connecting rods. The velocity of the two compressing pistons is given in Fig.7.

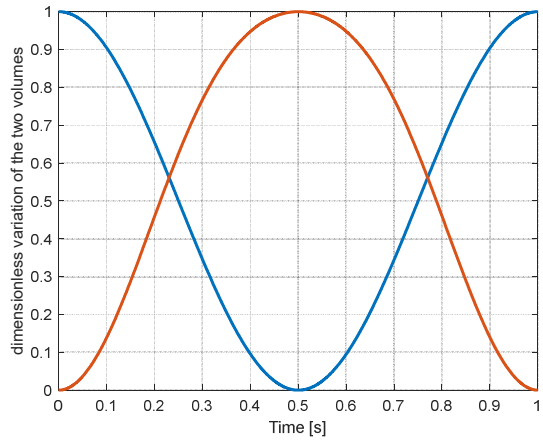

Fig. 6 Dimension-less variation of the volumes of the compression cylinders

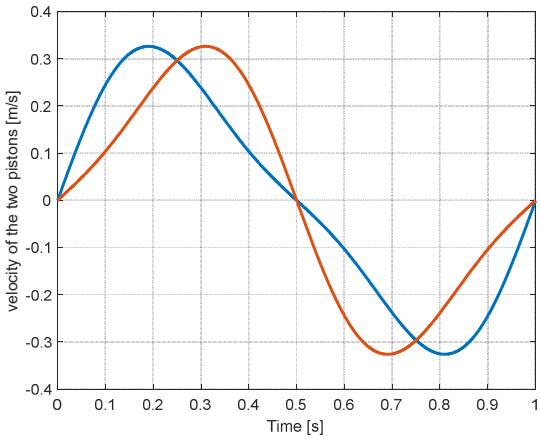

Fig. 7 Velocity of the pistons (m/s)

Figure 8 shows the evolution of the horizontal force of the left-side piston caused by the pressure in this cylinder. During the left-to-the-right stroke (0 to 0.5s), the diagram shows the force related to the pressure rise from the inlet pressure (15 bar) to the output pressure (160 bar). The elevation of the pressure is determined by a law of adiabatic evolution according rel. 15.

$$P_{gas} = P_{in\_gas}\left(\frac{V_{compr\_\mathrm{var}}}{V_{comp\_\max}}\right)^{\gamma} \quad \text{with } \gamma = 1.4 \tag{15}$$

During the second half-period (0.5s to 1s) which corresponds to the right-to-the-left stroke, the pressure level corresponds to the intake pressure (15 bar). The global force developed by the two pistons of the compression cylinders is represented in Fig. 9. One can see that the force components due to the intake pressure compensates partially the compression forces.

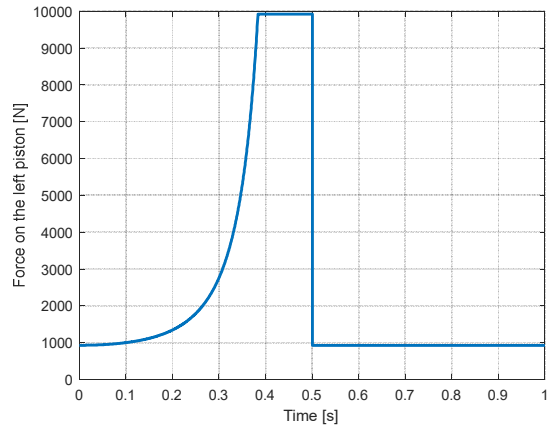

Fig. 8 Force developed by the left-side piston (N)

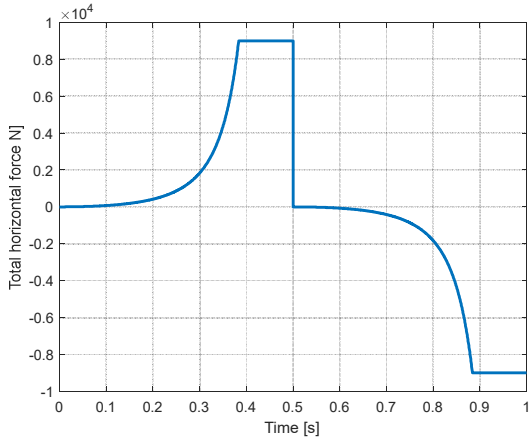

Fig. 9 Total force (horizontal) (N)

Figure 7 has shown the evolution of the piston's velocity. This information is further used to calculate the power developed by the compression cylinders (Fig. 10). This figure shows an interesting property of the system driven by a crankshaft and connecting rods, where the power (as well as the torque, see Fig.11) takes a negative value at the beginning of the compression phenomena. This effect is due to the asymmetrical evolution of the displacement and speed of the left and right cylinders. The value of the torque is obtained from the value of the powers according to relation 6.

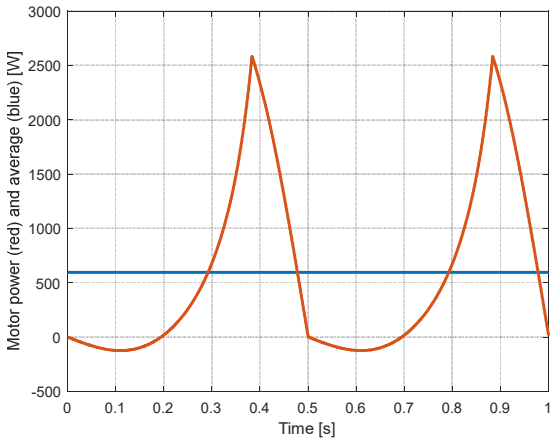

Fig. 10 Power received by the two pistons (W)

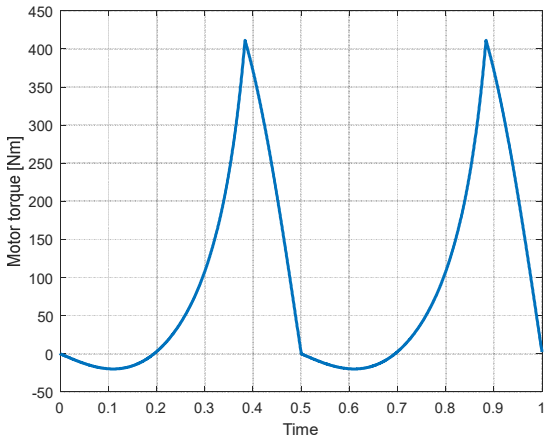

Fig. 11 Torque developed (crankshaft) (Nm)

The electric drive with an active power smoothing circuit

The waveforms of power and torque needed for the activation of the compression cylinders are represented in Fig. 10 and 11. These waveforms can be followed by a modern electric drive, for example a permanent magnet synchronous motor fed by a voltage source inverter. The power however should not be taken directly from the feeding grid where the power level is normally smooth. To obtain at the line side a fully smoothed power, a power compensating storage device is added and interconnected at the level of the intermediary DC circuit of the converter.

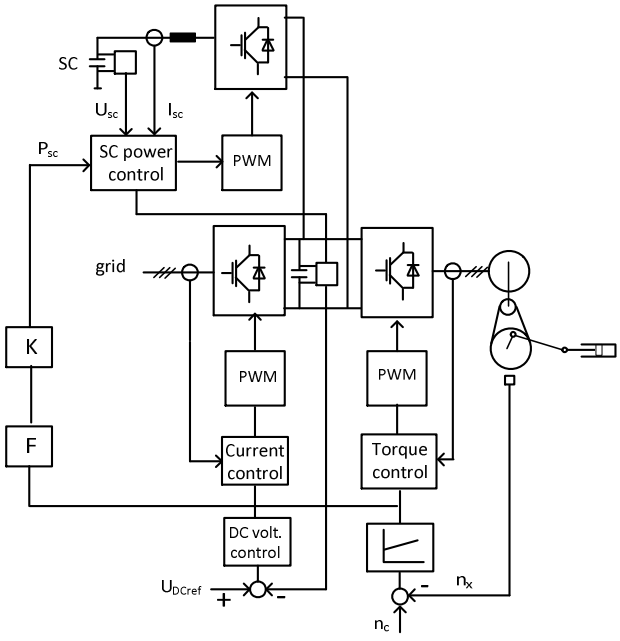

Fig. 12 Schematic diagram of the electric drive system with active power compensation circuit.

The active compensation device is composed of a capacitor which is periodically charged and discharged through a dedicated DC-DC conversion stage. The complete circuit of the drive fed by the voltage source converter and the active compensation circuit is represented in Fig. 12. The more detailed scheme of the power electronic circuits is given in Fig. 13.
The motor feeding converter is composed of two back-to-back connected voltage source converters. The two converters have at the motor-side a torque and speed controller, and at the line side a line current control with a superimposed DC-link voltage control (Fig. 12).

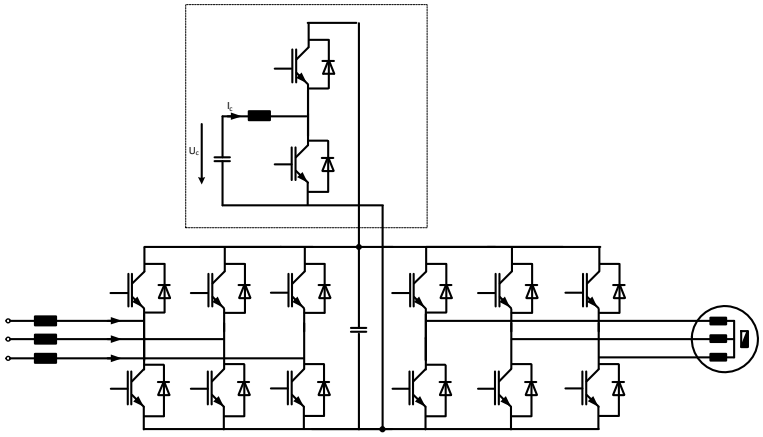

Fig. 13 Detailed scheme of the power electronic converter with active power compensation

According to the very specific waveform of the needed power and torque for the compression stages (Fig. 10 and 11), the driving motor current shows very strong variations. These variations and especially their corresponding low frequency can be seen in Fig. 14
The active power compensator is composed of a bidirectional step-down and step-up chopper circuit interfaced with the variable voltage storage capacitor and connected directly to the DC link of the frequency converter.

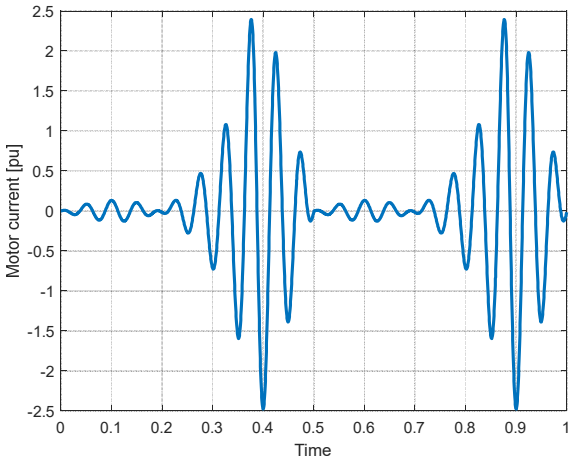

Fig. 14 Current in one phase of the motor (p.u)

The control of the active power compensator can be seen globally in Fig. 12. This control is based on the principle using a feed-forward power control signal obtained from the output of the speed controller at the motor side. Then, the control of the capacitor current is realized, taking in account the actual value of the capacitor voltage. The capacitor current reference is obtained by dividing the compensation power reference by the capacitor voltage. The detailed control circuit of the compensation capacitor is given in Fig. 15.

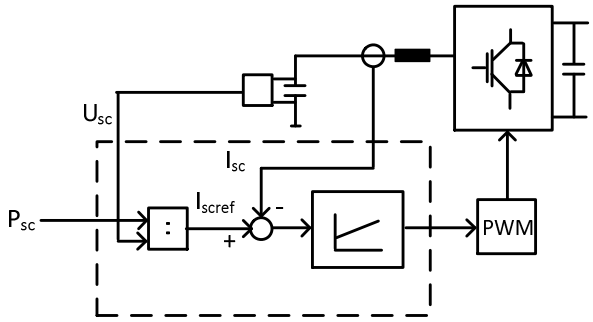

Fig. 15 Detailed scheme of the control of the compensation Capacitor

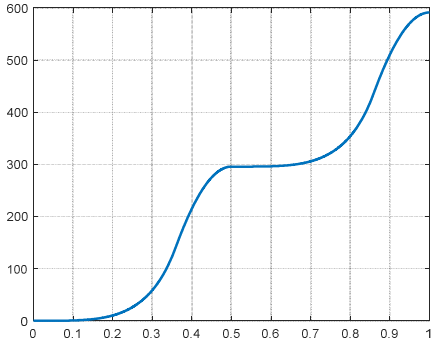

Fig. 16 Energy flow from the motor to the compression cylinders (J)

Design of the storage capacitor

The design of the storage capacitor is done on the base of the amount of energy to be stored and unstored in it. Fug. 16 illustrates the integral of the power, corresponding of the total energy flow.
During one cycle of the power which corresponds to one half of the revolution of the crankshaft, the energy variation is of 298 J. During this variation, the storage capacitor is charged and discharged in order to obtain a smooth average value at the level of the power exchange with the grid. The amounts of charged energy and of the discharged one are identic, and are equal to the half of the energy variation mentioned before

$$W_{Cch} = W_{Cdisch} = \frac{E_{\text{var}}}{2} = 298J / 2 = 149J \tag{16}$$

The domain of use of the capacitor in terms of its discharge ratio [9] can be calculated. The design criterion of this element corresponds to the definition of its corresponding voltage variation. The capacitor is discharged from its 100% value down to a value of 50%, starting from a physical value of 600V.
The total energy content of the fully charged capacitor is

$$W_{Ctot} = \frac{1}{2} C \cdot U^2 \tag{17}$$

And for a voltage variation from 100% to 50% the energy extracted is

$$W_{extr\_50} = \frac{1}{2} C \cdot (U^2 - \left(\frac{U}{2}\right)^2) = \frac{3}{4} \cdot \frac{1}{2} CU^2 \tag{18}$$

Then, the value of the capacitor is defined from

$$149J = \frac{3}{4} \cdot \frac{1}{2} CU^2$$

$$C = 149J \frac{4}{3} \cdot \frac{2}{U^2} = 149J \frac{4}{3} \cdot \frac{2}{(600V)^2} = 0.00110F \tag{19}$$

or 1100 µF

The waveform of the capacitor current of the active power compensation circuit is given in Fig. 17. The corresponding value of the capacitor voltage is represented in Fig. 18.

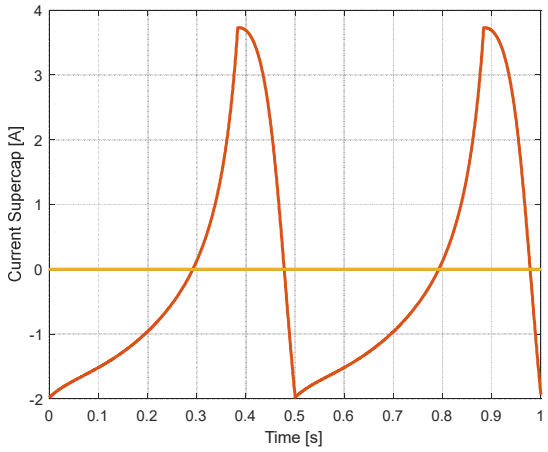

Fig. 17 Current exchanged with the compensator capacitor (A)

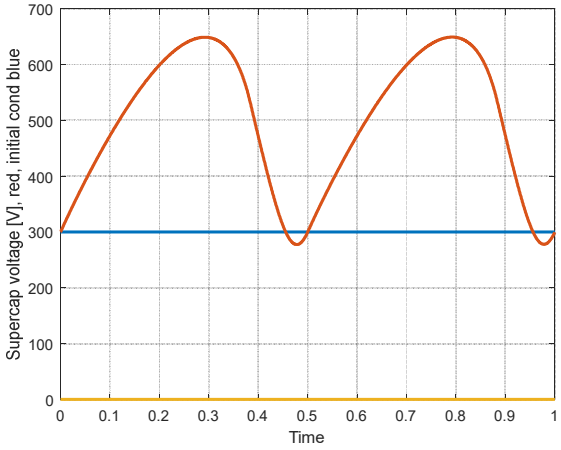

Fig. 18 Voltage of the storage capacitor (V)

Conclusions

An original electrically driven gas booster system is proposed as an alternative to the classical air-driven compressors where the energetic efficiency is problematic. A geared electric drive is proposed for delivering the strongly pulsating power demanded by the compression stages. Further, these power pulsations are compensated by an active storage circuit based on a controlled variable voltage capacitor. The paper has shown the characteristic waveform of the compressor forces, torque and pulsating power demand and proposed a design for the active power compensator. The power circuits are described together with their control functions.

References

[1] Ligen Y., Vrubel H., Arlettaz J., Girault H., Experimental correlations and integration of gas boosters in a hydrogen refueling station, International Journal of Hydrogen Energy, 45, (2020),16663-16671, Elsevier.

[2] Vito Gianfranco Truglia, High-Efficiency Engine Driven by Pressurized Air or Other Compressible Gases, Patent No US 9.677.400 B2, Jun. 13, 2017.

[3] Nègre Guy, Engine with an active mono-enery and/or bi-energy chamber with compressed air and/or additional energy and thermodynamic cycle thereof, US Patent US 7,469,527 B2, Dec. 30, 2008.

[4] Rufer A., A High efficiency pneumatic drive system using vane-type semi-rotary actuators, FACTA UNIVERSITATIS, Series: Electronics and Energetics, Vol. 34, Iss. 3, September 2021.

[5] Rufer A., Pneumatic cylinder assembly with enhanced energetic efficiency, PCT Patent application PCT/CH2021000002, May, 4th 2021.

[6] Yan Shi, Maolin Cai, Flow Characteristics of Expansion Energy Used Pneumatic Booster, Chinese Journal of Mechanical Engineering, Vol. 25, No. 5, 2012

[7] Rufer A., A pneumatic driven hydrogen compressor with reduced air consumption, Patent applications, 2021.

[8] George H Martin, Kinematics and Dynamics of machines, Mc Graw Hill Series in Mechanical Engineering, Waveland Press USA.

[9] Rufer A., Energy storage – Systems and components, CRC Press, Taylor and Francis group,2018